



Redescription and Molecular Characterization of *Pachysentis canicola* Meyer, 1931 (Acanthocephala: Oligacanthorhynchidae) from the Maned Wolf, *Chrysocyon brachyurus* (Illiger, 1815) in Texas

Omar M. Amin¹ · Anshu Chaudhary² · Richard A. Heckmann³ · Julie Swenson⁴ · Hridaya S. Singh²

Received: 11 June 2021 / Accepted: 20 July 2021 / Published online: 3 August 2021
© Witold Stefański Institute of Parasitology, Polish Academy of Sciences 2021

Abstract

Background The original description of *Pachysentis canicola* Meyer, 1931 was based on an unknown number of specimens from an undetermined species of *Canis* in Brazil from the Berlin Museum. It has since been reported from other carnivores in South and North America. Our specimens from the maned wolf, *Chrysocyon brachyurus* (Illiger, 1815), in Texas, represent a new host record, and has shed more light on morphometric characteristics missing from the original description, and expanded the range of variations in characters that remained fixed since 1931 and that have been repeated in other taxonomic accounts. We have found additional specimens in striped skunk, *Mephitis mephitis* Schreber, also in Texas.

Methods We have performed metal analysis on hooks using EDXA (energy dispersive X-ray analysis). Sequences for the *18S* gene and *ITS1-5.8-ITS2* region of rDNA were generated to molecularly characterize the species for the first time.

Results Worms with a massive trunk and a globular proboscis with prominent dome-like apical organ and 12 irregular spiral rows of 4–5 hooks deeply embedded in cuticular folds each, totaling 48–60 hooks. We have included line drawings of the male and female reproductive systems, among other structures, also missing from the original and subsequent descriptions. We describe a new population of *P. canicola* from Texas and report on the metal analysis of its hooks using EDXA. We also assess the phylogenetic position of *P. canicola* supporting its independent status in the family Oligacanthorhynchidae, inferred from the two molecular markers.

Conclusions This is the foremost molecular characterization of any species of *Pachysentis* and will provide significant insights and reference for future molecular study of species of *Pachysentis*, especially from this newly described Texas population.

Keywords Acanthocephala · Wolf · Molecular profile · Texas · *Pachysentis* · *18S* · *ITS1-5.8-ITS2*

Richard A. Heckmann—deceased.

✉ Omar M. Amin
omaramin@aol.com

- ¹ Institute of Parasitic Diseases, 11445 E. Via Linda 2-419, Scottsdale, AZ 85259, USA
- ² Molecular Taxonomy Laboratory, Department of Zoology, Chaudhary Charan Singh University, Meerut, U.P. 250004, India
- ³ Department of Biology, Brigham Young University, 1114 MLBM, Provo, UT 84602, USA
- ⁴ Fossil Rim Wildlife Center, 2155 County Road 2008, Glen Rose, TX 76043, USA

Introduction

Meyer [1] described *Pachysentis canicola* from an unknown number of specimens collected by Olfers and Sello from an undetermined species of “*Canis*” in Brazil deposited in the Berlin Museum. That description was repeated verbatim in Meyers [2] and Petrochenko [3]. Van Cleave [4] expanded on the measurements of trunk, proboscis, and eggs in specimens from various species of foxes and skunks from Texas and Oklahoma and provided line drawings of 8 proboscides showing variations in shape and armature. The unknown number of specimens studied by Van Cleave was obtained from gray fox, *Urocyon cinereoargenteus scotti* Mearns, striped skunk, *Mephitis m. mesomelas* Lichtenstein, Western hog-nosed skunk, *Conepatus mesoleucus* (Lichtenstein), Western spotted skunk, *Spilogale gracilis leucoparia* Merriam, and *Mephitis* sp. The gray

fox, *Urocyon cinereoargenteus texensis* Mearns, was also reported infected with *P. canicola* in eastern Texas with a high prevalence of 40% [5]. The tentative identification of specimens by Lucker as *P. canicola* “was later confirmed by Van Cleave” who recognized it as “the first record of occurrence of the genus *Pachysentis* on the North American continent” [5]. Three species of skunks, American hog-nosed skunk, *Conepatus leuconotus* Lichtenstein, striped skunk, *M. mephitis* (Schreber), and Western spotted skunk, *S. gracilis* (Merriam), were infected (prevalences of 46–78%) with *P. canicola* in west-central Texas [6]. Five specimens of *P. canicola* were recovered from a single coyote, *Canis latrans mearnsi* Merriam, in Southern Arizona [7]. Specimens of *P. canicola* were also deposited in the National Museum of American History (Behring Center), Washington, D.C., from 3 additional host species including raccoons, *Procyon lotor* (Linn.), in Texas (USNPC 098227.00; Van Cleave 3807), ring-tail cat, *Bassaricus astutus* Lichtenstein, in Texas (USNPC 098228.00; Van Cleave 3809), and the gray fox *Urocyon cinereoargenteus seattli* Schreber, in central Texas (USNPC 098224.00; Van Cleave 3757). Our collection from the maned wolf, *Chrysocyon brachyurus* (Illiger), represents a new host record; the thirteenth in North America.

Very little is known about the life history of this acanthocephalan. Snakes and possibly lizards apparently serve as paratenic hosts. Bolette [8] reported cystacanths of *P. canicola* in the serosal surface of the intestines and the liver and the mesenteries of western diamondback rattlesnakes, *Crotalus atrox* Baird and Girard (Serpentes: Viperidae), a paratenic host in Texas. Larvae of a related species of *Pachysentis*, *Pachysentis lenti* were found infecting the lizard *Ameiva ameiva ameiva* (Linn.) in the Brazilian Amazonia [9]. The long cylindrical specimens identified as *P. canicola* from red fox, *Vulpes vulpes* Linn., in Iran [10] are clearly misidentified.

We provide a revised description of *P. canicola* accounting for the noted variability in that species, completing missing information in the original and subsequent descriptions, and adding new information not observed by previous observers. Molecular data of *18S* gene and *ITS1-5.8-ITS2* region was generated but only those of *18S* were used. Moreover, its phylogenetic relationships with other members of Oligacanthorhynchida are analyzed and discussed.

Materials and Methods

Collections

Post mortem examination of two maned wolves a few years apart that were born at Fossil Rim Wildlife Center, Glen Rose, Texas (32°14'12"N, 97°45'14"W) showed significant infections with acanthocephalans. The first captive

8.5-year old male maned wolf with suspected inflammatory bowel disease (IBD) and confirmed intestinal lymphoma was euthanized in September, 2015. In December, 2018, about 50 adult worms were found in the jejunum during gross necropsy of another 8.5-year old maned wolf. Similar adult worms were subsequently found in the feces of 4 other maned wolves, as well as from a skunk, *Mephitis mephitis* Schreber, in the vicinity. Of the other 4 maned wolves, 3 were apparently healthy young animals. All 4 animals were confirmed to be passing adult acanthocephalans intermittently in the feces, mostly in the fall. Eggs were monitored in fecal exams and acanthocephalan eggs were also confirmed intermittently from all 4 animals. Clinical details of these infections are described by Haeefe et al. [11]. Many worms were collected but only about 25 that were placed in cold water for a few days before fixing in cold 70% ethanol were considered appropriate and selected for processing at our Arizona facility for further studies. A total of 22 whole worms were available: 10 worms were processed for microscopy in Scottsdale, Arizona, 8 whole worms and 4 half worms for SEM in the Provo, Utah facility, and 2 for molecular analysis in Meerut, India.

Methods for Microscopical Studies

Ten whole worms were punctured with a fine needle and subsequently stained in Mayer's acid carmine, destained in 4% hydrochloric acid in 70% ethanol, dehydrated in ascending concentrations of ethanol (24 h each), and cleared in 100% xylene then in 50% Canada balsam and 50% xylene (24 h each). Because of the thickness and toughness of the body wall, some worms were cut in 2 or 3 longitudinal sections to expose internal structures then chemically processed like the whole worms (above) for microscopical examination. Whole worms and sections were then mounted in Canada balsam. Measurements are in micrometers, unless otherwise noted; the range is followed by the mean values between parentheses. Width measurements represent maximum width. Trunk length does not include proboscis, neck, or bursa. Microscope images were created using a BH2 light Olympus microscope (Olympus Optical Co., Osachishibamiya, Okaya, Nagano, Japan) and an AmScope 1000 video camera (United Scope LLC, dba AmScope, Irvine, California), linked to an ASUS laptop equipped with HDMI high definition multimedia interface system (Taiwan-USA, Fremont, California). Other images (Figs. 5, 6) were created using a Sony Alpha a6000 Mirrorless Camera and Neewer LED video light (NL480, Shenzhen Neewer Technology Co., Ltd, Shenzhen, China).

SEM (Scanning Electron Microscopy)

Samples of parasites that had been fixed and stored in 70% ethanol were processed following standard methods [12] which included critical point drying in sample baskets and mounted on SEM sample mounts (stubs) using conductive double-sided carbon tape. Samples were coated with gold and palladium for 3 min using a Polaron #3500 sputter coater (Quorum [Q150 TES] www.quorumtech.com) establishing an approximate thickness of 20 nm. Samples were placed and observed in an FEI Helios Dual Beam Nanolab 600 (FEI, Hillsboro, Oregon) SEM with digital images obtained in the Nanolab software system (FEI) and then transferred to a USB for future reference. Images were taken at various magnifications. Samples were received under low vacuum conditions using 10 kV, spot size 2 0.7 Torr using a GSE detector.

X-Ray Microanalysis, EDXA (Energy Dispersive X-Ray Analysis)

Standard methods were used for preparation similar to the SEM procedure. Specimens were examined and positioned with the above SEM instrument which was equipped with a Phoenix energy-dispersive x-ray analyzer (FEI). X-ray spot analysis and live scan analysis were performed at 16 kV with a spot size of 5 and results were recorded on charts and stored with digital imaging software attached to a computer. The TEAM *(Texture and Elemental Analytical Microscopy) software system (FEI) was used. The data included weight percent and atom percent of the detected elements following correction factors.

Ion Sectioning of Hooks

A dual-beam SEM with a gallium (Ga) ion source (GIS) was used for the LIMS (Liquid Ion Metal Source) part of the process. The hooks of the acanthocephalans were sectioned using a probe current between 0.2 and 2.1 nA according to the rate at which the area is cut. The time of cutting is based on the nature and sensitivity of the tissue. Following the initial cut, the sample also goes through a milling process to obtain a smooth surface. The cut was then analyzed for chemical ions with an electron beam (Tungsten) to obtain an X-ray spectrum. The intensity of the GIS was variable due to the nature of the material being cut.

Molecular Methods

Total genomic DNA of the worm was extracted from 2 (95% ethanol) preserved specimens using DNeasy™ Blood and Tissue kit (Qiagen, Hilden, Germany) according to the manufacturer's instructions. Extracted DNA was amplified by

PCR reactions in a 25 µl reaction mixture using the primer pairs: 18SU467F (5'-ATCCAAGGAAGGCAGCAGGC-3'), 18SL1310R (5'-CTCCACCAACTAAGAACGGC-3') [13] for *18S* gene; and BD1 (5'-GTCGTAACAAGGTTTCCGTA-3') and BD2 (5'-TATGCTTAAATTCAGCGGGT-3') [14] for *ITS1 + 5.8S + ITS2* region. PCR reactions were performed in a volume of 25 µl and the PCR products were purified with the Purelink™ Quick Gel Extraction and PCR Purification Combo Kit (Invitrogen, Carlsbad, California). Amplification products were then sequenced with the Big Dye Terminator v3.1 cycle sequencing kit in ABI 3130 Genetic Analyzer (Applied Biosystems, Foster City, California). In the phylogeny, rDNA sequences amplified only *18S* region was used for analysis because the *ITS1 + 5.8S + ITS2* region can give a better result if other species of *Pachysentis* are available for comparison which is not the case, as it is unsuitable for comparison of distantly related taxa.

Sequences obtained during the study for *18S* region of *P. canicola* were manually edited using BioEdit, version 7.2.5 [15]. BLASTn search (<http://blast.ncbi.nlm.nih.gov/>) was used and compared for similarities with sequences from GenBank for *18S* available in GenBank (see Table 1) For *18S* molecular marker, sequences were aligned separately using the software Clustal W [16]. Maximum likelihood (ML) and Bayesian inference (BI) methods were used for phylogenetic analyses conducted using MEGA ver. 6.0 [17] and Topali 2.5 [18] respectively. For each molecular marker, a nucleotide substitution model was selected using jModel Test ver. 2.1.7 [19] applying the Akaike criterion and GTR + G + I were chosen as the best nucleotide substitution models for both data sets. For the ML analysis, 1000 bootstrap replicates were run to test for reliability in MEGA v. 6.0. The Maximum Likelihood analysis yielded best tree with a likelihood value (lnL) = -4828.076, the proportion of invariable sites = 0.21 and the gamma shape parameter = 0.46. For Bayesian inference (BI) analyses, the substitution models were tested by the Bayesian Information Criterion and GTR + G + I was chosen. Posterior probabilities were estimated using the Markov Chain Monte Carlo technique (MCMC) over 1,000,000 generations via 5 independent runs of 4 simultaneous Markov chains with every 100th tree saved. The “burn in” was set to 25%. The sequences of *18S* and *ITS1 + 5.8S + ITS2* of rDNA were submitted to the Genbank database. Sequences of *Lecane bulla* and *Brachionus diversicornis* (Rotifer) were used as outgroup for 18S analysis (Table 1).

Results

The present material was assigned to the genus *Pachysentis* Meyer [1] using the keys to the genera of Oligacanthorhynchidae by Schmidt [20] and Nickol and Dunagan

Table 1 Acanthocephalan species represented in the phylogenetic analysis with their host, GenBank accession numbers, locations and references

Species	Host	GenBank Accession no. 18S	Location	References
<i>Macracanthorhynchus ingens</i>	<i>Procyon lotor</i>	AF001844	USA	Near et al. [23]
<i>Macracanthorhynchus hirudinaceus</i>	<i>Sus scrofa leucomystax</i>	LC350001	Japan	Kamimura et al. [24]
<i>Macracanthorhynchus hirudinaceus</i>	<i>Sus scrofa leucomystax</i>	LC350002	Japan	Kamimura et al. [24]
<i>Pachysentis canicola</i> ^a	<i>Chrysocyon brachyurus</i>	MT864728	USA	Present study
<i>Pachysentis canicola</i> ^a	<i>Chrysocyon brachyurus</i>	MT864729	USA	Present study
<i>Oncicola</i> sp.	<i>Nasua narica</i>	AF064818	Mexico	García-Varela et al. [25]
<i>Oligacanthorhynchus tortuosa</i>	<i>Didelphis virginiana</i>	AF064817	Mexico	García-Varela et al. [25]
<i>Moniliformis moniliformis</i>	<i>Rattus rattus</i>	HQ536017	Spain	Foronda Rodriguez et al. (Unpublished)
<i>Moniliformis</i> sp. RPE-2016	<i>Paraechinus aethiopicus</i>	KU206782	Saudi Arabia	Amin et al. [26]
<i>Moniliformis cryptosaudi</i>	<i>Hemiechinus auritus</i>	MH401043	Iraq	Amin et al. [27]
<i>Moniliformis kalahariensis</i>	<i>Atelerix frontalis</i>	MH401042	South Africa	Amin et al. [27]
<i>Mediorhynchus</i> sp.1 RPE-2013	<i>Numida meleagris</i>	KC261353	South Africa	Amin et al. [28]
<i>Mediorhynchus gallinarum</i>	NA	KC261354	Indonesia	Amin et al. [28]
<i>Mediorhynchus grandis</i>	<i>Sturnella magna</i>	AF001843	USA	Near et al. [23]
<i>Neoechinorhynchus cylindricus</i>	<i>Micropterus salmoides</i>	MF974925	USA	Blubaugh and Gauthier (Unpublished)
<i>Neoechinorhynchus crassus</i>	<i>Catostomus commersoni</i>	AF001842	USA	Near et al. [23]
<i>Polyacanthorhynchus caballeroi</i>	<i>Caiman yacare</i>	AF388660	Bolivia	García-Varela et al. [29]
<i>Polymorphus obtusus</i>	<i>Aythya affinis</i>	JX442172	Mexico	García-Varela et al. [30]
<i>Echinorhynchus gadi</i>	NA	AY218123	USA	Giribet et al. [31]
<i>Pseudoacanthocephalus toshimai</i>	<i>Rana pirica</i>	LC129278	Japan	Nakao [32]
<i>Pseudoacanthocephalus lucidus</i>	<i>Rana ornativentris</i>	LC129279	Japan	Nakao [32]
<i>Dentitruncus truttae</i>	<i>Salmo trutta</i>	JX460863	Croatia	Irena et al. [33]
<i>Koronacantha mexicana</i>	<i>Pomadasys leuciscus</i>	AY830157	USA	García-Varela and Nadler [34]
<i>Brachionus diversicornis</i> (outgroup)	NA	MK106113	China	Wang (Unpublished)
<i>Lecane bulla</i> (outgroup)	NA	DQ297698	USA	Sørensen and Giribet [35]

NA not available

^aThis species is sequenced in the present study

[21], and the key to the 10 valid species of *Pachysentis* by Gomes et al. [22], as well as materials and specimens in the Amin collection. The results of the morphometric observations compared to those of Meyer [1] and Van Cleave [4] are listed in Table 2. Line drawings of the male and female reproductive systems, among other structures, complete measurements of hooks, receptacle, lemnisci, testes, cement glands, and Saefftigen's pouch, SEM images, and EDXA are provided for the first time. The following description is based on the specimens recovered from maned wolves in Texas. Qualitative characters are similar to those in the description of Meyer [1]. However, new and modified qualitative observations are included in our description. Measurements and quantitative observations are included in Table 2 in comparison with those of Meyer [1] and Van Cleave [4].

Morphological Description

Pachysentis canicola Meyer, 1931 [1] (Figs. 1, 2, 3, 4, 5, 6, 7, 8, 9, 10, 11, 12, 13, 14, 15, 16, 17, 18, 19, 20, 21)

General With characters of the genus *Pachysentis* and the family Oligacanthorhynchidae as emended by Van Cleave (1953). Body and common structures markedly larger in females than in males. Trunk massive, stout, straight ventrally but convex dorsally, broader near the middle or anteriorly, with transverse grooves along lacunar canals appearing beady in cross-sections along dorsal and ventral sides of the body wall. Anterior-most trunk bent ventrad (Figs. 1, 2, 3, 5, 6). Body wall with many fragmented nuclei and electron-dense micropores varying in diameter and distribution along trunk length (Figs. 13, 14). Proboscis somewhat globular,

Table 2 Morphometric comparisons among specimens of *Pachysentis canicola* in the original description by Meyer (1931), Van Cleave (1953), and ours from the United States

Reference	Meyer (1931)	Van Cleave (1953)	Present paper
Host	“ <i>Canis</i> ” <i>Spilogale leucoparia</i>	<i>Urocyon</i> spp., <i>Mephitis mesomelas</i> , <i>Conepatus mesoleucas</i>	<i>Chrysocyon brachyurus</i>
Locality	Brazil	Texas and Oklahoma	Texas
Sample size	–	–	5 males, 5 females
<i>Males</i>			
Trunk $L \times W$ (mm)	15.0 × 4.0	15.0–28.0 × 4.0–8.0	14.0–30.0 (20.0) × 2.9–4.5 (3.9) ^a
Proboscis $L \times W$	800 × 850	570–800 × 570–800	577 × 570
Hook rows × H/row	6 × 4 + 12 × 4 (total 72 hooks)	12 diagonal rows × 6 (up to 72 sometimes) ^b	12 diagonal rows × 4–5 (48–60 hooks)
Longest hook L	–	173–346	154
Prob. Recep. $L \times W$ (mm)	2.0 × –	–	1.5 × 0.6
Lemnisci $L \times W$ (mm)	7.0 × –	–	3.0–4.1 (3.6) × 0.4–0.6 (0.5)
Lemniscal nuclei	5	–	6
Ant. Testis $L \times W$ (mm)	2.0 × –	–	2.0–3.7 (2.7) × 0.7–1.2 (1.0)
Post. Testis $L \times W$ (mm)	2.0 × –	–	2.0–2.7 (2.3) × 0.7–1.2 (0.9)
Cement gl. $L \times W$ (mm)	3.0 × – (8 gl. together)	–	0.9–1.4 (1.3) × 0.5–1.12 (0.8)
Saeffligen’s p. $L \times W$ (mm)	–	–	1.7–2.2 (2.0) × 0.4–0.9 (0.6)
<i>Females</i>			
Trunk $L \times W$ (mm)	20.0–26.0 × 5.0	20.0–26.0 × 5.0–11.0	14.0–33.0 (24.5) × 3.7–8.0 (6.1)
Proboscis $L \times W$	800 × 850	570–800 × 570–800	520–680 (600) × 620–680 (640)
Hook rows × H/row	6 × 4 + 12 × 4 (total 72 hooks)	12 diagonal spirals × 6 (up to 72 sometimes)	12 diagonal rows × 4–5 (48–60 hooks)
Longest hook L	–	346	176
Prob. Recep. $L \times W$ (mm)	2.0 × –	–	1.3–1.6 (1.5) × 0.5–0.8 (0.7)
Lemnisci $L \times W$ (mm)	7.0 × –	–	3.7–4.6 (4.3) × 0.3–0.5 (0.4)
Lemniscal nuclei	5	–	6
Reprod. Syst. L (mm)	–	–	2.0
Eggs $L \times W$	70 × 40–45	58–72 × 38–45	62–73 (65) × 36–52 (46)

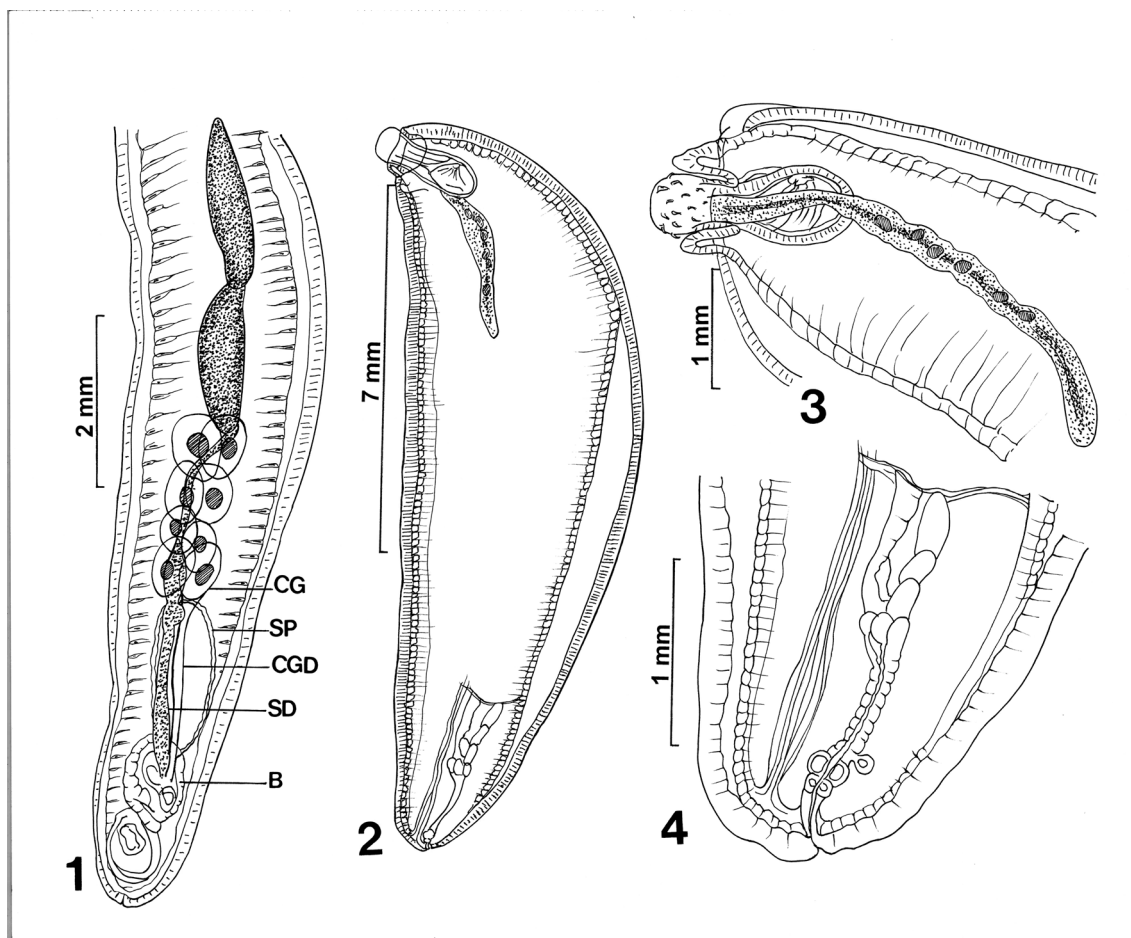
^aRange (mean) in μm unless otherwise stated

^bFigures 102–106 and 114–116 of Van Cleave’s (1953) show proboscides with estimated 60–68 hooks each Bolette (1997) counted 56 hooks in 12 rows of 4–5 hooks each

about as long as wide, with a prominent dome-like apical organ and 12 irregular spiral rows of 4–5 hooks each totaling 48–60 hooks (Figs. 7, 8, 9). Hooks smooth, not ribbed or barbed, progressively decrease in size posteriorly, partially embedded in elevated cuticular boat-like heavy rims especially prominent anteriorly (Figs. 10, 11, 12). Anterior hooks largest, with anteriorly directed roots (Fig. 19); posterior hooks rootless. Proboscis receptacle about three times as long as proboscis, rounded posteriorly, double-walled, with thick inner wall inserted inside proboscis just anterior to basal hooks. Cerebral ganglion prominent, just posterior to middle of receptacle, lateral, near the point of passage of retractor muscles into the body cavity (Fig. 3). Neck short but distinct. Four sensory pores on proboscis just anterior to basal hooks and 2 others in neck. Lemnisci is relatively

long, flat, band-like, with central channel and 6 ameoboid giant nuclei. Gonopore terminal in males and dorso-terminal in females (Figs. 1, 2, 15, 16).

Males Based on 5 whole mounted mature adults, 4 longitudinally cut halves, and 4 specimens used for SEM. See Table 2 for measurements. Testes elongate-ovoid, occasionally bluntly pointed ends, contiguous, slightly pre-equatorial. Cement glands large, round, 8 in 4 pairs, with 1 large spherical giant nucleus each, overlapping anteriorly with posterior testis and posteriorly with anterior margin on large, ovoid, well-developed Saeffligen’s pouch. Two sperm ducts passing through cement glands and joining into common sperm duct at the junction of posterior cement glands and Saeffligen’s pouch then draining posteriorly into bursa.



Figs. 1–4 Line drawings of specimens of *Pachysentis canicola* from *Chrysocyon brachyurus* in Texas. (1) The posterior half of a male specimen showing the reproductive system. Note the nucleated cells on the dorso-lateral sides marking the pattern of transverse grooves of the lacunar system. The sperm duct from the anterior testis is hidden behind the posterior testis and only the sperm duct from the posterior testis is shown. Only 1 cement gland duct is shown. B: bursa; CG: cement gland; CGD: cement gland duct; SD: common sperm duct; SP: Saeftigen's pouch. (2) A whole female specimen showing the trunk shape and relative proportions of the receptacle, lemnisci and reproductive system. Note the beady appearance of the lacunar

channels in cross-sections at the dorsal and ventral inner body wall. Crowded ovarian balls, not shown, obscured the second lemniscus. (3) A higher magnification of the anterior end of a worm showing the rounded posterior end of the receptacle and its insertion into the proboscis and the relative size of and central groove in the lemniscus. The second lemniscus was obscured by ovarian balls; not shown. (4) A female reproductive system of a worm showing the dorso-terminal gonopore and the ventral para-vaginal bundle of fibers. Protonephridial capsule at top of the uterine bell masked by many ovarian balls that are not shown (1–4)

Cement gland ducts passing posteriorly along the common sperm duct to drain into bursa (Figs. 1, 20).

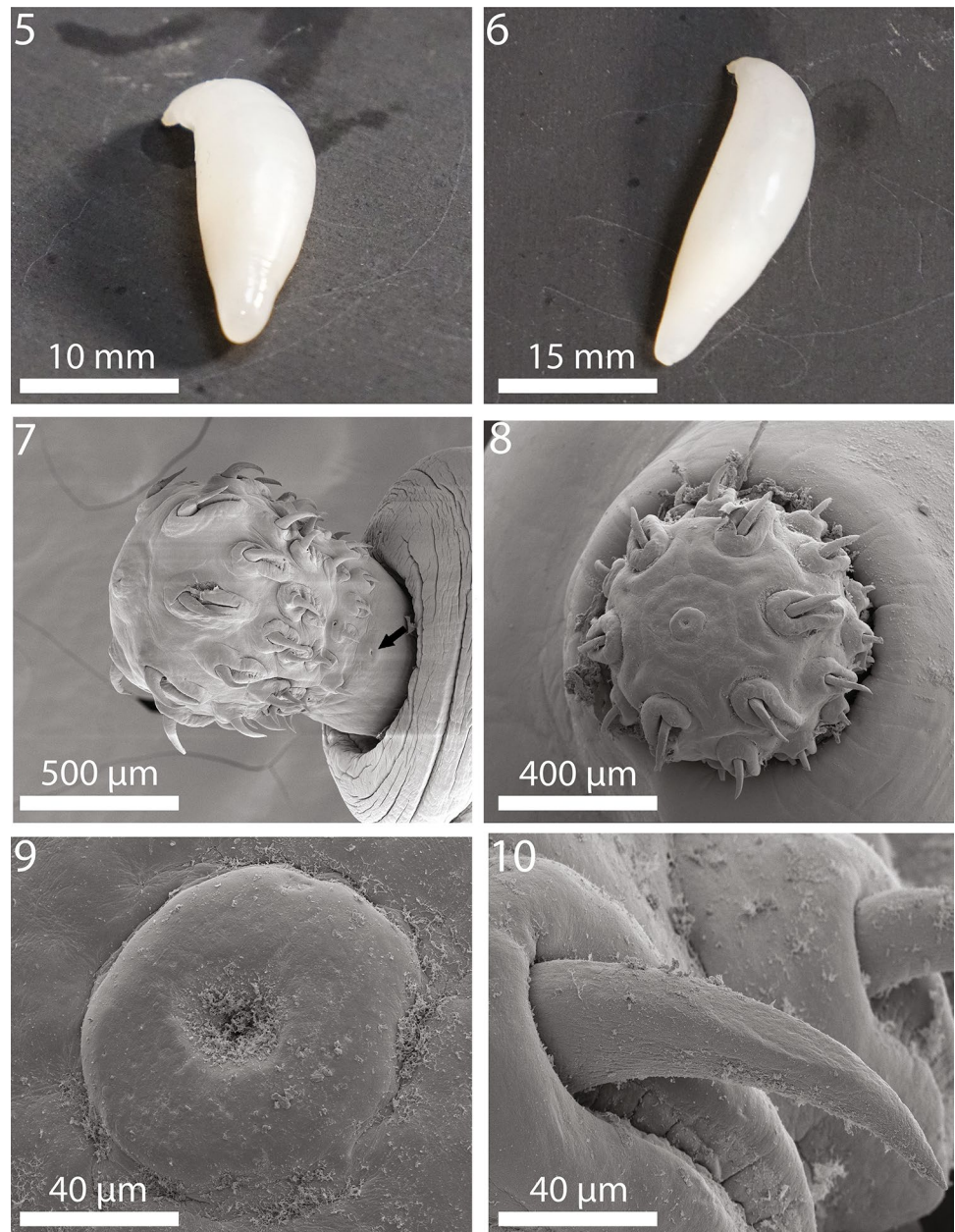
Females Based on 5 whole mounted mature adults, 3 longitudinally cut halves, and 3 specimens used for SEM. See Table 2 for measurements. Reproductive system about one-fourth length of the trunk with specialized longitudinal bundle of para-vaginal fibers on the ventral side opposite reproductive system opening dorsotermally. Paired vaginal bulbs setting deeper inside trunk, uterus and uterine bell moderately developed. Uterus thick with an undulating wall, prominent out-pouch basally, and few anterior cells. Uterine bell chunky with few thick cells and wavy

anterior end associated with transverse connective tissue joining it with body wall dorsally and with para-vaginal fibers ventrally (Figs. 2, 4, 21). Capsular protonephridial organ is attached to the anterior end of the uterine bell but masked by ovarian balls. Eggs ovoid, compact, with concentric membranes and thick outer shell becoming extremely thin at poles (Figs. 17, 18, 21).

Taxonomic Summary

Type host: “*Canis*” (Meyer, 1931)

Figs. 5–10 Images of specimens of *Pachysentis canicola* from *Chrysocyon brachyurus* in Texas. **(5)** A whole male worm. **(6)** A female worm. **(7–10)** SEM images. **(7)** A lateral view of a proboscis. Note the sensory pores on the partially extruded neck and on the posterior proboscis. **(8)** An apical view of a proboscis showing its ornate pattern, the central apical organ pore, and the alternating 12 rows of hooks. **(9)** A high magnification of the apical organ of another proboscis showing its dome-shaped appearance and deeply recessed pore. **(10)** An anterior hook deeply recessed in thick boat-like cuticular fold (5–10)



Hosts in our study: *Chrysocyon brachyurus* (Illiger, 1815), *Mephitis mephitis* (Schreber). See introduction for other hosts.

Type locality: Brazil.

Other locality in our study: Fossil Rim Wildlife Center, Glen Rose, Texas (32°14'12"N, 97°45'14"W).

Site of infection: intestine.

Material deposited: six whole mounted specimens on slides were deposited at the HWML coll. No. 216343.

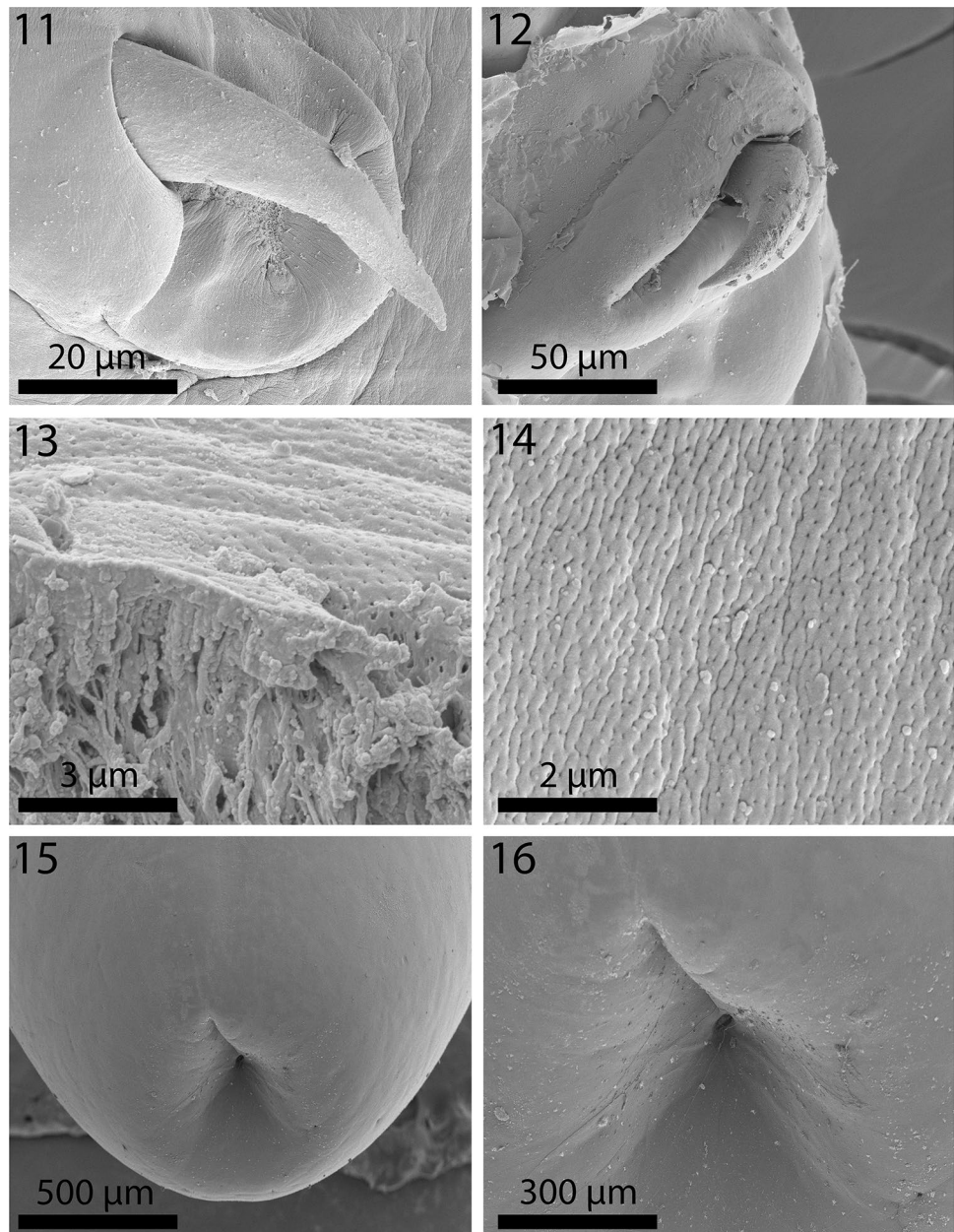
Representative sequence: the *18S* gene and *ITS-5.8-ITS2* region of rDNA sequences of *P. canicola* were deposited in the GenBank under the accession numbers

MT864728 (900 bp), MT864729 (890 bp) for *18S* gene and MT864730 (710 bp), MT864731 (707 bp) for *ITS* region.

Micropores

Micropores covered the whole trunk of female specimens of *P. canicola* and cut-up sections of the body wall showed the associated canalicular system (Figs. 13, 14). These observations are consistent with our findings commonly observed in other species of acanthocephalans.

Figs. 11–16 SEM of specimens of *Pachysentis canicola* from *Chrysocyon brachyurus* in Texas. **(11, 12)** Middle and posterior hooks, respectively. All hooks are deeply recessed within heavy boat-like cuticular folds. **(13)** Micropores on the surface of the mid-trunk of a worm (top) and a cut-up section of the body wall (below) showing the crypts and canaliculi associated with the micropores. **(14)** The micropores at the cuticular surface of the mid trunk of a worm. **(15)** The posterior end of a female specimen showing the near-terminal position of the gonopore. **(16)** A higher magnification of the female genital orifice (11–16)



Energy Dispersive X-Ray Analysis (EDXA)

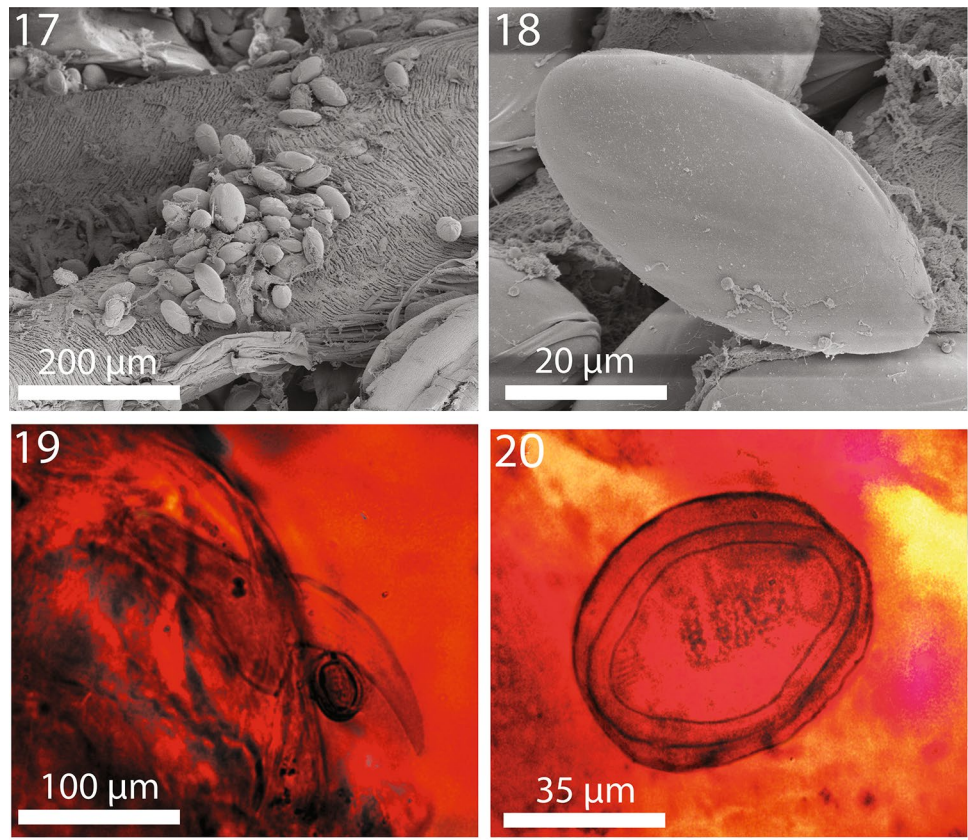
The results of the EDXA of anterior hooks of *P. canicola* show low levels of Calcium (1.18% of weight) and Phosphorus (1.67%) and negligible traces of Sulphur (0.09%). The Magnesium level was negligible at 0.22% but the Sodium level at 1.21% was comparable to that of the Calcium (Table 3). The first 3 elements are directly associated with the hardness of hooks. No other analyses have been conducted for other species of *Pachysentis* so comparisons of the chemical profile of hooks could not be made. A baseline for future comparisons is, however, established.

Phylogenetic Analysis

The specimens of *P. canicola* presented amplification of *18S* and *ITS1-5.8-ITS2* region of rDNA. But here in this study, we presented only the analysis of *18S* gene as it is more informative including data from families Oligacanthorhynchidae, Moniliformidae and Gigantorhynchidae mainly within the clade originated for Archiacanthocephala while some species of Eoacanthocephala and Palaeacanthocephala were also included in the analysis (Table 1).

Our phylogeny based on *18S* region inferred using ML and BI methods resulted in similar topologies

Figs. 17–20 SEM and microscope images of specimens of *Pachysentis canicola* from *Chrysocyon brachyurus* in Texas. **(17)** Eggs suspended on the ribbed epithelium of the uterus. **(18)** A high magnification of 1 egg. Note the smooth surface and the lack of any special ornamentation or fibrils. **(19–20)** Microscope images. **(19)** The anterior corner of a proboscis showing an anterior hook and its root with large anterior manubrium. **(20)** A ripe egg. Note the thin polar ends of the outer shell (17–20)



with variations in bootstrap/posterior probabilities values (Fig. 21). *Pachysentis canicola* isolates show no intraspecific sequence variability. The sequence of *P. canicola* in the 18S analysis formed a well-supported group with other species of family Oligacanthorhynchidae (ML = 90, BI = 0.91). The intergeneric divergence of *P. canicola* with *M. ingens*, *M. hirudinaceus*, *Oncicola* sp. and *Oligacanthorhynchus tortuosa* of family Oligacanthorhynchidae ranged between 0.3% and 0.5%. The class Archiacanthocephala shows monophyly with strong support (ML = 99, BI = 1.00) as also mentioned in previous studies [29]. The family Oligacanthorhynchidae was found sister to the family Moniliformidae, though with low support (ML = 76, BI = 0.8). The group formed by sequences of *P. canicola* suggested it as a sister group formed by sequences of *Macracanthorhynchus* (ML = 80, BI = 0.85) and *Oncicola* (ML = 90, BI = 0.91) with moderate to good support respectively. An inclusion, *Oligacanthorhynchus tortuosa* formed a group sister to other archiacanthocephalans with weakly supported by ML (84) and is not supported by BI (Fig. 21). Moreover, among the members of the tree including Archiacanthocephala, *Mediorhynchus* sp. (Gigantorhynchidae) is placed at the basal position.

Discussion

Micropores

Micropores are present throughout the epidermal surface of the trunk of *P. canicola* like those reported in other species of the Acanthocephala. They are associated with internal crypts and vary in diameter and distribution in different trunk regions corresponding with differential absorption of nutrients. We have documented this phenomenon in 16 species of acanthocephalans [36] and a few more since. The functional aspects of micropores in a few other acanthocephalan species including *Rhadinorhynchus ornatus* Van Cleave, 1918, *Polymorphus minutus* (Goeze, 1782) Lühe, 1911, *Moniliformis moniliformis* (Bremser, 1811) Travassos (1915), *Macracanthorhynchus hirudinaceus* (Pallas, 1781) Travassos (1916, 1917), and *Sclerocolum rubrimaris* Schmidt and Paperna, 1978 were reviewed earlier by Amin et al. [37]. The peripheral canals of the micropores are continuous with canalicular crypts that constitute a huge increase in external surface area implicated in nutrient up take [38, 39]. Whitfield [40] estimated a 44-fold increase at a surface density of 15 invaginations

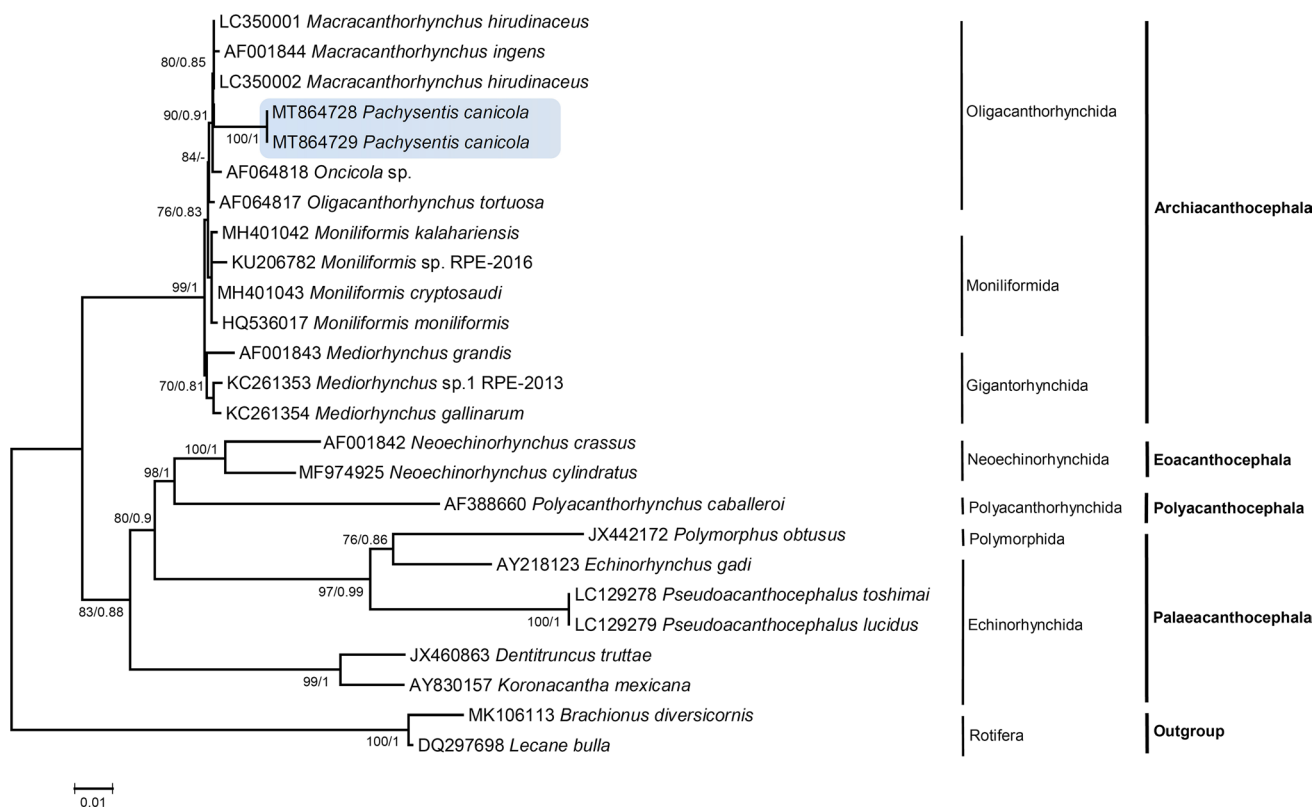


Fig. 21 Phylogenetic relationship of *Pachysentis canicola* with closely related sequences available on GenBank. The tree is inferred from the 18S rRNA sequences using maximum likelihood (ML) and Bayesian Inference (BI) method. Both the ML and BI methods pro-

duced the same branch topologies. Nodal support for ML and BI indicated as ML/BI. Hyphen indicates node unsupported by BI. GenBank accession numbers are provided alongside the species names. The scale-bar indicates the number of substitutions per site

per 1 μm² of *Moniliformis moniliformis* (Bremser, 1811) Travassos, 1915 tegumental surface. The micropores and the peripheral canal connections to the canaliculi of the inner layer of the tegument were demonstrated by transmission electron micrographs in *Corynosoma strumosum* (Rudolphi, 1802) Lühe, 1904 from the Caspian seal *Pusa caspica* (Gmelin) in the Caspian Sea (figs. 19, 20 of Amin et al. 2011 [41]) and in *Neoechinorhynchus personatus*

Tkach et al. [42] from *Mugil cephalus* Linn. in Tunisia (Figs. 26, 29, 30 in Amin et al. 2020 [43]).

Energy Dispersive X-Ray Analysis (EDXA)

Our studies of acanthocephalan worms have usually involved X-ray scans (EDXA) of gallium cut hooks and other hard worm structures [44–46]. Hooks are evaluated for chemical ions with Sulfur (S), Calcium (Ca) and Phosphorus (P) being the prominent elements for the hardening of hooks. Sulfur is usually seen at the outer edge of large hooks and Calcium and Phosphorus are major ions in the base and middle of hooks. All 3 elements were surprisingly present at notably low or negligible levels indicating the weakness of the hooks of *P. canicola* which appears to be the chemical signature of hooks of that species (Table 3). Large hooks normally play a major role in host tissue attachment. For example, in *Cavisoma magnum* (Southwell, 1927) Van Cleave, 1931 from *Mugil cephalus* in the Arabian Sea, unusually high levels of Sulfur in hook tips (43.51 wt%) and edges (27.46 wt%) were found. The center and base of hooks of the same worms had negligible Sulfur levels and contained mostly Phosphorus (15.02–21.44%) and Calcium (31.76–39.30%),

Table 3 Chemical composition of hooks of *Pachysentis canicola* from a skunk in Texas

Element ^a	Anterior hook
Sodium (Na)	1.21
Magnesium (Mg)	0.22
Silicon (Si)	0.35
Phosphorus (P)	1.67
Sulfur (S)	0.09
Calcium (Ca)	1.18

A whole mount scan of anterior hook

^aCommon protoplasmic elements (C, N, O) and processing elements (Au, Pd, Ga) omitted. Reported in wt%

the two other essential elements in hook structure [47]. It is assumed that the Sulfur ions are found in the disulfide bonds linking the amino acid cysteine in the hardened protein of the outer hook layer. These bonds are in conjunction with Ca and P to establish the hardened apatite. This is similar to the tooth enamel of mammals. Variable amounts of Sulfur could account for the hardened nature of the hook. Raynaud et al. [48] using X-ray diffraction, demonstrated that the increased stability of protein (such as in the proboscis hook) is due to the amount of disulfide bonds in the product using X-ray diffraction.

In *C. magnum*, the magnesium level at hook base (1.66%) was greater than that of *P. canicola* (0.22%) but the Sodium level was dramatically higher at 14.13% compared to 1.21% in *P. canicola*. Mg probably plays a role in the mineralization of hooks similar to that of the disulfide bonds formed by S in the protein apatite; its diminished level in *P. canicola* corresponds with the poor levels of Ca and P in the same species. The above described EDXA pattern of the hard parts of this species sets up its chemical personality.

Like fingerprints, the EDXA appears to be species-specific and has significant diagnostic value in acanthocephalan systematics [49]. For example, *Moniliformis cryptosaudi* Amin et al., 2019 was erected based primarily on its EDXA pattern [27]. Our results demonstrate very low levels of all chemicals essential for the hardness of hooks (Table 3). No other species of *Pachysentis* or related genera were available to make comparisons. The present findings will provide a baseline for future comparisons with species of *Pachysentis*. Our methodology for the detection of the chemical profile of hooks in the Acanthocephala has also been used in other parasitic groups including the Monogenea [50, 51] and Cestoda [52].

Phylogenetic Analysis

The present study helps to resolve the phylogenetic relationship of *Pachysentis canicola* since this is the first molecular data available which predicts the placement of it with other members of the family Oligacanthorhynchidae and other closely related families in the tree. The estimated interspecific divergences among the *P. canicola* and other species of the family Oligacanthorhynchidae was based on both partial 18S rDNA region being 0.2–0.4% respectively. Phylogenetic analysis based on 18S rDNA shows a close relationship of *P. canicola* with species of *Macracanthorhynchus* while demonstrating the distinct separation of the family Oligacanthorhynchidae from the closely related families Moniliformidae and Gigantorhynchidae. This study also indicates that the family Oligacanthorhynchidae is sister to Moniliformidae although with low support. Regarding the status of the family Oligacanthorhynchidae, we suggested that it is not monophyletic but more genetic data and thorough studies are

required to resolve the relationships in the future. Moreover, our phylogenetic analyses agree with previous studies that Archiacanthocephala is monophyletic. Additionally, according to previous studies, Polyacanthocephala seems to form a sister group with Eoacanthocephala and well separated from Palaeacanthocephala [29].

This is the first species of *Pachysentis* that is molecularly characterized as no molecular data is available in other parts of the world. So, wider taxonomic and geographical sampling of *Pachysentis* species is necessary to assess the genetic diversity for a better understanding of the phylogenetic affinities and systematic position of the species in this genus.

Acknowledgements This project was supported by the Department of Biology, Brigham Young University (BYU), Provo, Utah, and by an Institutional Grant from the Parasitology Center, Inc. (PCI), Scottsdale, Arizona. We thank Madison Laurence, Bean Museum (BYU) and Nataliya Rubtsova (PCI) for expert help in the preparation and organization of plates and figures and to Michael Standing, Electron Optics Laboratory (BYU), for his technical help and expertise. We would like to acknowledge the laboratory facilities provided by the Department of Zoology, Chaudhary Charan Singh University, Meerut, India. The authors would also like to thank the staff at Fossil Rim Wildlife Center, Glen Rose, Texas, especially Dr. Holly Haefele and Allyssa Roberts, LVT, for procuring the specimens that were used for this project as well as to thank Dr. Michael Kinsella (HelmWest Laboratory, Missoula, Montana) and Dr. Michael Garner (Northwest Zoo Path, Monroe, Washington) for their assistance with their original recognition of these parasites as acanthocephalans.

Declarations

Conflict of interest The authors declare that they have no conflict of interest.

Ethical Approval The authors declare that they have observed all applicable ethical standards.

References

1. Meyer A (1931) Neue Acanthocephalen aus dem Berliner Museum. Burggründung eines neue Acanthocephalen systems auf Grund einer Untersuchung der Berliner Sammlung. Zoologische Jahrbücher Abteilung für Systematik, Ökologie und Geographie der Tiere 62: 53–108. (in German)
2. Meyer A (1933) Acanthocephala. In: Bronn's Klassen und Ordnungen des Tierreichs. Vol. 4. Akademische Verlagsgesellschaft, Leipzig, Germany, Bd. 4, 2 Abt., 2 Buch, pp 333–582. (in German)
3. Petrochenko VI (1958) Acanthocephala of domestic and wild animals. Isdatel'stvo Akad. Nauk SSSR, Moscow, Russia. (English translation by Israel Program for Scientific Translations, 1971, p 478)
4. Van Cleave HJ (1953) Acanthocephala of North American mammals III. Biol Monogr 23:1–79
5. Buechner HK (1944) Helminth parasites of the gray fox. J Mammal 25:185–188
6. Neiswenter SA, Pence DB, Dowler RC (2006) Helminths of sympatric striped, hog-nosed, and spotted skunks in West-Central

- Texas. *J Wildl Dis* 42:511–517. <https://doi.org/10.7589/0090-3558-42.3.511>
7. Drewek J Jr (1980) Behavior, population structure, parasitism, and other aspects of coyote ecology in southern Arizona. Ph.D. dissertation. University of Arizona, Tucson, Arizona, pp 261
 8. Bolette DP (1997) First record of *Pachysentis canicola* (Acanthocephala: Oligacanthorhynchidae) and the occurrence of *Mesocostoides* sp. *Tetrathyridia* (Cestoidea: Cyclophyllidea) in the western diamondback rattlesnake, *Crotalus atrox* (Serpentes: Viperidae). *J Parasitol* 83:751–752
 9. Macedo LC, De Vasconcelos Melo FT, Ávila-Pires TCS, Giese EG, Dos Santos JN (2016) Acanthocephala larvae parasitizing *Ameiva ameiva ameiva* (Linnaeus, 1758) (Squamata: Teiidae). *Rev Bras Parasitol Vet* 25:119–123. <https://doi.org/10.1590/S1984-29612016007>
 10. Mobedi I, Mowlavi Gh, Rahno A, Turner Mobedi K, Mojaradi A (2007) Natural infection of *Pachysentis canicola* (Acanthocephala: Oligacanthorhynchidae) in fox from Persian Gulf coastal area in Iran. *Iran J Parasitol* 2:44–47
 11. Haefele HJ, Swenson J, Kinsella M, Amin OM, Garner M (2020) Acanthocephalans in captive maned wolves (*Chrysocyon brachyurus*). American Association of Zoo Veterinarians 52nd Annual conference (virtual), Nashville, Tennessee, 20–24 Sept 2020
 12. Lee RE (1992) Scanning electron microscopy and X-ray microanalysis. Prentice Hall, Englewood Cliffs, p 458
 13. Suzuki N, Hoshino K, Murakami K, Takeyama H, Chow S (2008) Molecular diet analysis of phyllosoma larvae of the Japanese spiny lobster *Palinurus japonicus* (Decapoda: Crustacea). *Mar Biotechnol* 10:49–55. <https://doi.org/10.1007/s10126-007-9038-9>
 14. Galazzo DE, Dayanandan S, Marcogliese DJ, McLaughlin JD (2002) Molecular systematics of some North American species of *Diplostomum* (Digenea) based on rDNA-sequence data and comparisons with European congeners. *Can J Zool* 80:2207–2217. <https://doi.org/10.1139/z02-198>
 15. Hall TA (1999) BioEdit: a user-friendly biological sequence alignment editor and analysis program for Windows 95/98/NT. *Nucleic Acids Symp Ser* 41:95–98
 16. Thompson JD, Higgins DG, Gibson TJ (1994) CLUSTAL W: improving the sensitivity of progressive multiple sequence alignment through sequence weighting, position-specific gap penalties and weight matrix choice. *Nucleic Acids Res* 22:4673–4680. <https://doi.org/10.1093/nar/22.22.4673>
 17. Tamura K, Stecher G, Peterson D, Filipksi A, Kumar s, (2013) MEGA6: molecular evolutionary genetics analysis version 6.0. *Mol Biol Evol* 30:2725–2729. <https://doi.org/10.1093/molbev/mst197>
 18. Milne I, Lindner D, Bayer M, Husmeier D, Mcguire G, Marshall DF, Wright F (2009) TOPALiv2: a rich graphical interface for evolutionary analyses of multiple alignments on HPC clusters and multi-core desktops. *Bioinformatics* 25:126–127. <https://doi.org/10.1093/bioinformatics/btn575>
 19. Posada D (2008) jModelTest: phylogenetic model averaging. *Mol Biol Evol* 25:1253–1256. <https://doi.org/10.1093/molbev/msn083>
 20. Schmidt GD (1972) Revision of the class Archiacanthocephala Meyer, 1931 (Phylum Acanthocephala), with emphasis on Oligacanthorhynchidae Southwell et Macfie, 1925. *J Parasitol* 58:290–297
 21. Nickol BB, Dunagan TT (1989) Reconsideration of the acanthocephalan genus *Echinopardalis*, with a description of adult *E. atrata* and a key to genera of the Oligacanthorhynchidae. *Proc Helminthol Soc Wash* 56:8–13
 22. Gomes APN, Amin OM, Olifiers N, de Bianchi CR, Souza JGR, Barbosa HS, Maldonado A Jr (2019) A new species of *Pachysentis* Meyer, 1931 (Acanthocephala: Oligacanthorhynchidae) in the brown-nosed coati *Nasua nasua* (Carnivora: Procyonidae) from Brazil, with notes on the genus and a key to species. *Acta Parasitol* 64:587–595. <https://doi.org/10.2478/s11686-019-00080-6>
 23. Near JT, Garey JR, Nadler SA (1998) Phylogenetic relationships of the acanthocephala inferred from 18S ribosomal DNA sequences. *Mol Phylogenet Evol* 10:287–298. <https://doi.org/10.1006/mpev.1998.0569>
 24. Kamimura K, Yonemitsu K, Maeda K, Sakaguchi S, Setsuda A, Varcasia A, Sato H (2018) An unexpected case of a Japanese wild boar (*Sus scrofa leucomystax*) infected with the giant thorny-headed worm (*Macracanthorhynchus hirudinaceus*) on the mainland of Japan (Honshu). *Parasitol Res* 117:2315–2322. <https://doi.org/10.1007/s00436-018-5922-7>
 25. García-Varela M, Pérez-Ponce de León G, de la Torre P, Cummings MP, Sarma SSS, Lacleste JP (2000) Phylogenetic relationships of Acanthocephala based on analysis of 18S ribosomal RNA gene sequences. *J Mol Evol* 50:532–540
 26. Amin OM, Heckmann RA, Osama M, Evans RP (2016) Morphological and molecular descriptions of *Moniliformis saudi* sp. n. (Acanthocephala: Moniliformidae) from the desert hedgehog, *Paraechinus aethiopicus* (Ehrenberg) in Saudi Arabia, with a key to species and notes on histopathology. *Folia Parasitol* 26:63. <https://doi.org/10.14411/fp.2016.014>
 27. Amin OM, Heckmann RA, Sharifdini M, Albayati NY (2019) *Moniliformis cryptosaudi* n. sp., (Acanthocephala: Moniliformidae) from the long-eared hedgehog *Hemiechinus auratus* (Gmelin) (Erinaceidae) in Iraq; a case of incipient cryptic speciation related to *M. saudi* in Saudi Arabia. *Acta Parasitol* 64:195–204. <https://doi.org/10.2478/s11686-018-00021-9>
 28. Amin OM, Evans P, Heckmann RA, El-Naggar AM (2013) The description of *Mediorhynchus africanus* n. sp. (Acanthocephala: Gigantorhynchidae) from galliform birds in Africa. *Parasitol Res* 112:2897–2906. <https://doi.org/10.1007/s00436-013-3461-9>
 29. García-Varela M, Cummings MP, Pérez-Ponce de León G, Gardner SL, Lacleste JP (2002) Phylogenetic analysis based on 18S ribosomal RNA gene sequences supports the existence of class polyacanthocephala (acanthocephala). *Mol Phylogenet Evol* 23:288–292. [https://doi.org/10.1016/S1055-7903\(02\)00020-9](https://doi.org/10.1016/S1055-7903(02)00020-9)
 30. García-Varela M, Pérez-Ponce de León G, Aznar FJ, Nadler SA (2013) Phylogenetic relationship among genera of Polymorphidae (Acanthocephala), inferred from nuclear and mitochondrial gene sequences. *Mol Phylogenet Evol* 68:176–184. <https://doi.org/10.1016/j.ympev.2013.03.029>
 31. Giribet G, Sørensen MV, Funch P, Kristensen RM, Sterrer W (2004) Investigations into the phylogenetic position of Micrognathozoa using four molecular loci. *Cladistics* 20:1–13. <https://doi.org/10.1111/j.1096-0031.2004.00004.x>
 32. Nakao M (2016) *Pseudoacanthocephalus toshimai* sp. nov. (Palaeacanthocephala: Echinorhynchidae), a common acanthocephalan of anuran and urodelan amphibians in Hokkaido, Japan, with a finding of its intermediate host. *Parasitol Int* 65:323–332. <https://doi.org/10.1016/j.parint.2016.03.011>
 33. Irena VS, Damir V, Damir K, Zrinka D, Emil G, Helena C, Emin T (2013) Molecular characterisation and infection dynamics of *Dentitruncus truttae* from trout (*Salmo trutta* and *Oncorhynchus mykiss*) in Krka River, Croatia. *Vet Parasitol* 197:604–613. <https://doi.org/10.1016/j.vetpar.2013.07.014>
 34. García-Varela M, Nadler SA (2005) Phylogenetic relationships of Palaeacanthocephala (Acanthocephala) inferred from SSU and LSU rDNA gene sequences. *J Parasitol* 91:1401–1409. <https://doi.org/10.1645/GE-523R.1>
 35. Sørensen MV, Giribet G (2006) A modern approach to rotiferan phylogeny: combining morphological and molecular data. *Mol Phylogenet Evol* 40:585–608. <https://doi.org/10.1016/j.ympev.2006.04.001>
 36. Heckmann RA, Amin OM, El Naggar AM (2013) Micropores of Acanthocephala, a scanning electron microscopy study. *Scientia Parasitol* 14:105–113

37. Amin OM, Heckmann RA, Radwan NA, Mantuano JS, Alcivar MAZ (2009) Redescription of *Rhadinorhynchus ornatus* (Acanthocephala: Rhadinorhynchidae) from skipjack tuna, *Katsuwonus pelamis*, collected in the Pacific Ocean off South America, with special reference to new morphological features. *J Parasitol* 95:656–664. <https://doi.org/10.1645/GE-1804.1>
38. Wright RD, Lumsden RD (1969) Ultrastructure of the tegumentary pore-canal system of the acanthocephalan *Moniliformis dubius*. *J Parasitol* 55:993–1003
39. Byram JE, Fisher FM Jr (1973) The absorptive surface of *Moniliformis dubius* (Acanthocephala). I Fine structure. *Tissue Cell* 5:553–579. [https://doi.org/10.1016/S0040-8166\(73\)80045-X](https://doi.org/10.1016/S0040-8166(73)80045-X)
40. Whitfield PJ (1979) The biology of parasitism: an introduction to the study of associating organisms. University Park Press, Baltimore, p 277
41. Amin OM, Heckmann RA, Halajian A, El-Naggar AM (2011) The morphology of an unique population of *Corynosoma strumosum* (Acanthocephala, Polymorphidae) from the Caspian seal, *Pusacaspica*, in the land-locked Caspian Sea using SEM, with special notes on Histopathology. *Acta Parasitol* 56:438–445. <https://doi.org/10.2478/s11686-011-0070-6>
42. Tkach I, Sarabeev V, Shvetsova L (2014) Taxonomic status of *Neoechinorhynchus agilis* (Acanthocephala, Neoechinorhynchidae), with a description of two new species of the genus from the Atlantic and Pacific mullets (Teleostei, Mugilidae). *Vestn Zool* 48:291–306. <https://doi.org/10.2478/vzoo-2014-0035>
43. Amin OM, Sharifdini M, Heckmann RA, Rubtsova N, Chine HJ (2020) On the *Neoechinorhynchus agilis* (Acanthocephala: Neoechinorhynchidae) complex, with the description of *Neoechinorhynchus ponticus* n. sp. from *Chelon auratus* Risso in the Black Sea. *Parasite* 27:48. <https://doi.org/10.1051/parasite/2020044>
44. Heckmann RA, Amin OM, Standing MD (2007) Chemical analysis of metals in acanthocephalans using energy dispersive X-ray analysis (EDXA, XEDS) in conjunction with a scanning electron microscope (SEM). *Comp Parasitol* 74:388–391. <https://doi.org/10.1654/4258.1>
45. Heckmann RA, Amin OM, Radwan NAE, Standing MD, Eggett DL, El Naggar AM (2012) Fine structure and energy dispersive X-ray analysis (EDXA) of the proboscis hooks of *Radinorynchus ornatus*, Van Cleave 1918 (Rhadinorynchidae: Acanthocephala). *Scientia Parasitol* 13:37–43
46. Standing MD, Heckmann RA (2014) Features of acanthocephalan hooks using dual beam preparation and XEDS phase maps. *Microscopy and Microanalysis Meeting: Hartford, Connecticut, Poster. Subm. No. 0383-00501*
47. Amin OM, Heckmann RA, Bannai M (2018) *Cavisoma magnum* (Cavisomidae), a unique Pacific acanthocephalan redescribed from an unusual host, *Mugil cephalus* (Mugilidae), in the Arabian Gulf, with notes on histopathology and metal analysis. *Parasite* 25:5. <https://doi.org/10.1051/parasite/2018006>
48. Raynaud S, Champion E, Benache-Assollant D, Thomas P (2000) Calcium phosphate apatites with variable Ca. P. atomic ratio synthesis, characterization and thermal stability of powder. *Biomaterials* 23:1065–1072. [https://doi.org/10.1016/s0142-9612\(01\)00218-6](https://doi.org/10.1016/s0142-9612(01)00218-6)
49. Amin OM, Chaudhary A, Heckmann RA, Ha NV, Singh HS (2019) The Morphological and Molecular Description of *Acanthogyryrus (Acanthosentis) fusiformis* n. sp. (Acanthocephala: Quadrigyridae) from the Catfish *Arius* sp. (Ariidae) in the Pacific Ocean off Vietnam, with Notes on Zoogeography. *Acta Parasitol* 64:779–796. <https://doi.org/10.2478/s11686-019-00102-3>
50. Rubtsova NYu, Heckmann RA, Smit WS, Luus-Powell WJ, Halajian A, Roux F (2018) Morphological studies of developmental stages of *Oculotrema hippopotami* (Monogenea: Polystomatidae) infecting the eye of *Hippopotamus amphibius* (Mammalia: Hippopotamidae) using SEM and EDXA with notes on histopathology. *Korean J Parasitol* 56:463–475. <https://doi.org/10.3347/kjp.2018.56.5.463>
51. Rubtsova NYu, Heckmann RA (2019) Structure and morphometrics of *Ancyrocephalus paradoxus* (Monogenea: Ancyrocephalidae) from *Sander lucioperca* (Percidae) in Czechia. *Helminthologia* 56:11–21. <https://doi.org/10.2478/helm-2018-0037>
52. Rubtsova NYu, Heckmann RA (2020) Morphological features and structural analysis of plerocercoids of *Spirometra erinaceieuropaei* (Cestoda: Diphyllbothriidae) from European pine marten, *Martes martes* (Mammalia: Mustelidae) in Ukraine. *Comp Parasitol* 87:100–117. <https://doi.org/10.1654/1525-2647-87.1.109>